CHEMISTRY
A European Journal
Communication

Main-Group Elements

Isolation of Carbene-Stabilized Arsenic Monophosphide [AsP] and its Radical Cation [AsP]+· and Dication [AsP]2+

Adinarayana Doddi,*[a] Dirk Bockfeld,[b] Marc-Kevin Zaretzke,[b] Thomas Bannenberg,[b] and Matthias Tamm*[b]

Abstract: Arsenic monophosphide (AsP) species supported by two different N-heterocyclic carbenes were prepared by reaction of (IDipp)PSiMe$_3$ (**1**) (IDipp = 1,3-bis(2,6-diisopropylphenyl)imidazolin-2-ylidene) with (IMes)AsCl$_3$ (**2**) (IMes = 1,3-bis(2,4,6-trimethylphenyl)imidazolin-2-ylidene) to afford the dichloride [(IMes)As(Cl)P(IDipp)]Cl (**3**), which upon reduction with KC$_8$ furnished heteroleptic [(IMes)AsP(IDipp)] (**4**). The corresponding mono- and dications [(IMes)AsP(IDipp)][PF$_6$], [**5**]PF$_6$ and [(IMes)AsP(IDipp)][GaCl$_4$]$_2$, [**6**][GaCl$_4$]$_2$, respectively, were prepared by one-electron oxidation of **4** with ferrocenium hexafluorophosphate, [Fc]PF$_6$ or by chloride abstraction from **3** with two equivalents of GaCl$_3$, respectively. Compounds **4**–**6** represent rare examples of heterodiatiomic interpnictogen compounds, and X-ray crystal structure determinations together with density functional theory (DFT) calculations reveal a consecutive shortening of the As–P bond lengths and increasing bond order, in agreement with the presence of an arsenic–phosphorus single bond in **4** and a double bond in **6**$^{2+}$. The EPR signal of the cationic radical [**5**]+· indicates a symmetric spin distribution on the AsP moiety through strong hyperfine coupling with the ^{75}As and ^{31}P nuclei.

IDipp = bis(2,6-diisopropylphenyl)imidazolin-2-ylidene) representing the most prominent examples. In contrast, heterodinuclear species are rare, and to the best of our knowledge, the heteroleptic carbene-stabilized "phosphorus mononitride" **A** and its radical cation (PN$^+$) represent the only compounds, in which a diatomic moiety consisting of two different p-block elements is supported by two carbene ligands (Figure 1).[8]
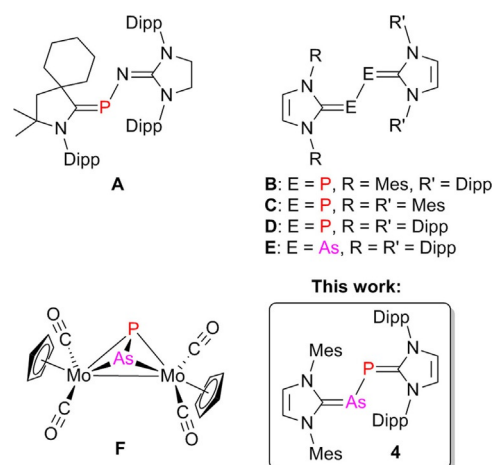

Figure 1. Examples of homo- and heterodinuclear dipnictogen compounds (Dipp = 2,6-diisopropylphenyl, Mes = 2,4,6-trimethylphenyl).

Carbene stabilization of diatomic allotropes has been among the most successful applications of N-heterocyclic carbenes (NHC) in main-group element chemistry,[1] with the homodinuclear systems [(IDipp)E$_2$(IDipp)] (E = B,[2] Si,[3] Ge,[4] Sn,[5] P,[6] As,[7]

[a] Dr. A. Doddi
Department of Chemical Sciences, Indian Institute of Science Education and Research Berhampur, Transit Campus, Govt. ITI Building
Engineering School Road, Ganjam, Berhampur, 760010, Odisha (India)
E-mail: adoddi@iiserbpr.ac.in

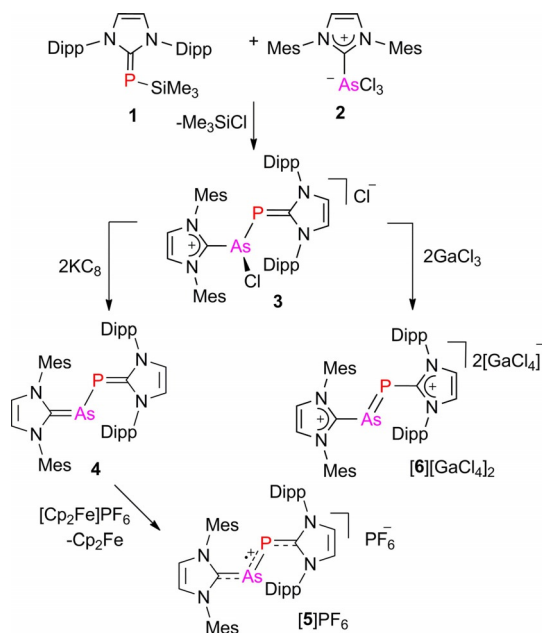[b] Dr. D. Bockfeld, M.-K. Zaretzke, Dr. T. Bannenberg, Prof. Dr. M. Tamm
Institut für Anorganische und Analytische Chemie
Technische Universität Braunschweig
Hagenring 30, 38106 Braunschweig, (Germany)
E-mail: m.tamm@tu-bs.de
Homepage: http://www.tu-braunschweig.de/iaac

The controlled synthesis of such species requires a modular approach for assembling the two different (NHC)E sides, and we have recently established such a protocol successfully for the preparation of the heteroleptic dicarbene–diphosphorus species [(IMes)P$_2$(IDipp)] (**B**, IMes = bis(2,4,6-trimethylphenyl)-imidazolin-2-ylidene),[9] which represents a hybrid of the previously reported homoleptic congeners [(IMes)P$_2$(IMes)] (**C**) and [(IDipp)P$_2$(IDipp)] (**D**).[6] Moreover, in a similar manner as described for **D** and also for the analogous diarsenic compound [(IDipp)As$_2$(IDipp)] (**E**),[10,11] the corresponding radical cation [(IMes)P$_2$(IDipp)]+· and dication [(IMes)P$_2$(IDipp)]$^{2+}$ were also prepared and structurally characterized. Notably, the heteroleptic nature of this system allowed for establishing phosphorus–phosphorus coupling in the diamagnetic neutral and dicationic forms.[9]

We reasoned that a similar modular approach could give access to heterodiatomic Group 15 species and therefore aimed at the isolation of carbene-stabilized arsenic monophosphide [(IMes)AsP(IDipp)] (**4**). Like homodinuclear P$_2$ and As$_2$,

the heterodinuclear AsP molecule was studied spectroscopically in the gas phase[12] or in solid neon matrix,[13] and a dissociation energy of 429.7(12.6) kJ mol^{-1} was determined by mass spectrometry. This energy falls between the values of 485.8(0.4) and 379.1(9.6) kJ mol^{-1} derived for P$_2$ and As$_2$, respectively.[14] In the solid state, arsenic monophosphide was found to crystallize in the orthorhombic crystal system,[15] and this black arsenic–phosphorus form has recently emerged as a promising candidate for two-dimensional electronic materials application.[16] AsP and other unsupported heterodiatomic Group 15 ligands were also stabilized in transition-metal complexes such as [Cp$_2$Mo$_2$(CO)$_4$(μ-η^2:η^2-PAs)] (**F**), which contains a Mo$_2$AsP tetrahedrane core.[17,18] Tetrahedral AsP$_3$ is another interpnictide molecule that has been employed as a ligand in coordination chemistry.[20,19]

The N-heterocyclic carbene–trimethylsilylphosphinidene adduct (IDipp)PSiMe$_3$ (**1**) served as an excellent synthon for the transfer of the (IDipp)P moiety by reaction with main-group element and transition-metal halides.[9,21] Likewise, the equimolar reaction of **1** with the NHC adduct of arsenic trichloride (IMes)AsCl$_3$ (**2**) at room temperature in toluene afforded the dichloro species **3** which was isolated as an orange solid in 79% yield and in pure form according to elemental analysis (Scheme 1).

Scheme 1. Preparation of heteroleptic N-heterocyclic carbene-supported AsP species.

The ^{31}P NMR spectrum (Figure S5, Supporting Information) of **3** in CD$_2$Cl$_2$, however, showed four different signals at 132.2, 20.3, 16.5, and 1.8 ppm at room temperature, indicating the presence of isomers with different chlorine binding modes (Scheme S1). Single crystals of **3**·3 CH$_2$Cl$_2$ were isolated from dichloromethane/hexane solution, and X-ray diffraction analysis revealed the formation of the ionic compound [(IMes)As(Cl)P-(IDipp)]Cl containing a chloride counterion and one chlorine
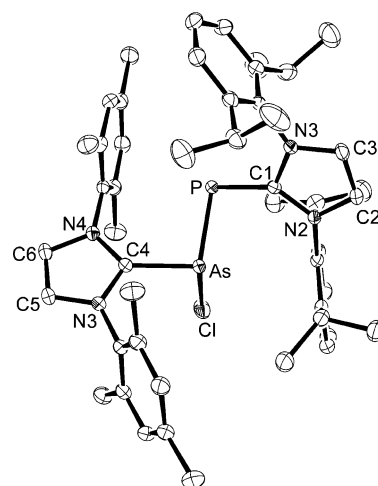
Figure 2. ORTEP diagram of the cationic part in [(IMes)As(Cl)P(IDipp)]Cl (**3**) with thermal displacement parameters drawn at 50% probability level. Hydrogen atoms are omitted for clarity. Selected bond lengths [Å] and angles [°]: As—P 2.2152(6), As—C4 1.9848(16), P—C1 1.8132(17); C1-P-As 93.64(6), C4-As-P 97.58(5), N3-C4-N4 106.28(14), N2-C1-N1 105.76(14).

atom bound to the arsenic atom (Figure 2). The As—P bond length is 2.2152(6) Å, which is almost identical with the As—P distances reported for the cationic C_2-symmetric compound [(IDipp)PAsP(IDipp)]Cl (2.203(1) Å)[22] and for the bimetallic AsP complex **F** (2.2324(13) Å).[17] Slightly longer bonds were found for other related NHC arsenic–phosphorus systems, for example 2.3133(4) Å in [(SIMes)PAs(*t*Bu)$_2$][23] or 2.3552(6) Å in the IDipp adduct of a transient phosphino–arsinidene (SIMes = 1,3-bis(2,4,6-trimethylphenyl)imidazolidin-2-ylidene).[24]

Reduction of **3** with two equivalents of potassium graphite (KC$_8$) in THF afforded [(IMes)AsP(IDipp)] (**4**) which was isolated as a dark red solid in 37% yield (Scheme 1). The ^{31}P NMR spectrum (in C$_6$D$_6$, Figure S8, Supporting Information) showed a broad signal at −60.6 ppm, which lies between the chemical shifts established for the homoleptic diphosphorus species [(IDipp)P$_2$(IDipp)] (**B**, −52.4 ppm) and [(IMes)P$_2$(IMes)] (−73.6 ppm),[6] whereas the heteroleptic congener [(IMes)-P$_2$(IDipp)] afforded two doublets with similar chemical shifts at −63.1 and −59.4 ppm ($^1J_{PP}$ = 249 Hz).[9] The ^{1}H NMR spectrum of **4** at room temperature shows the signals expected for the IMes and IDipp ligands, for instance at 5.83 and 6.00 ppm for the backbone imidazole CH hydrogen atoms; these signals are broadened, indicating slightly hindered rotation around the E—C bonds (E = P, As). In the ^{13}C NMR spectrum, two characteristic doublets are found for the carbene carbon atoms at 169.0 ppm ($^1J_{PC}$ = 112 Hz) and 171.0 ppm ($^2J_{PC}$ = 17 Hz).

The molecular structure of **4** was established by X-ray diffraction analysis (Figures 3 and 5), confirming the expected *trans*-bent geometry with a slightly twisted, but almost coplanar orientation of the imidazole rings towards the central AsP unit as indicated by torsion angles of 162.25(13)° (C1-P-As-C4), 179.38(19)° (N2-C1-P-As), and 172.91(18)° (N3-C4-P-As). The As—P bond length is 2.3149(8) Å,[25] which is consistent with an As—P single bond (2.32 Å)[26] and intermediate between the P—P distances in the corresponding diphosphorus systems, specif-
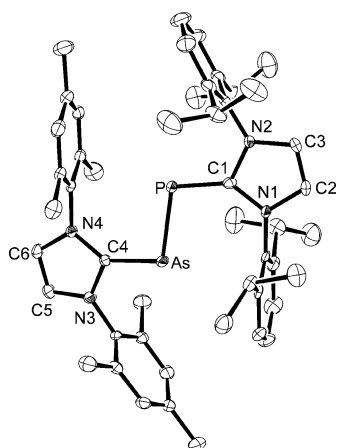
Figure 3. ORTEP diagram of [(IMes)AsP(IDipp)] (**4**) with the thermal displacement parameters drawn at 50 % probability level. Hydrogen atoms are omitted for clarity. Selected bond lengths [Å] and angles [°]: As—P 2.3149(8), As—C4 1.884(2), P—C1 1.750(3); As-P-C1 101.61(9), P-As-C4 100.40(8), N3-C4-N4 103.91(19), N1-C1-N2 103.3(2).

ically 2.1897(4) (**B**),[9] 2.1897(11) (**C**),[6] and 2.2052(10) Å (**D**),[6] as well as the As—As distance of 2.442(1) Å in the diarsenic compound **E**.[7] A virtually identical As—P bond length of 2.3133(4) Å was found for [(SIMes)PAs(*t*Bu)$_2$].[23] It also falls in the range established for other As—P single bonds, as for instance in cyclodiarsadiphosphanes,[27] or in complexes containing the tetrahedral AsP$_3$ ligand.[19,20] The phosphorus–carbon and arsenic–carbon bond lengths of 1.750(3) (P—C1) and 1.884(2) Å (As—C4) are well within the range established for carbene–pnictinidene adducts, for example 1.763(6) and 1.899(3) Å in (IMes)EPh (E = P, As)[28] or 1.752(1) and 1.883(2) Å in (IDipp)EH (E = P, As),[22,29] in agreement with the presence of polarized P—C and As—C double bonds.

It was previously demonstrated that the dicarbene-supported P$_2$ and As$_2$ species **D** and **E** can be oxidized stepwise to the respective radical cation and dications.[10,11] Accordingly, treatment of **4** with one equivalent of ferrocenium hexafluorophosphate ([Fc]PF$_6$) in THF afforded [(IMes)AsP(IDipp)]PF$_6$, [**5**]PF$_6$, as a dark green solid in 38 % yield (Scheme 1). Compound [**5**]PF$_6$ represents a rare example of a carbene-stabilized main-group radical species containing two different p-block elements,[30] and it was fully characterized by elemental analysis, EPR spectroscopy, and X-ray crystal-structure determination. The X-band EPR spectrum of a CH$_2$Cl$_2$ solution at room temperature is shown in Figure 4 (left); it shows a multiplet with an isotropic *g* value of 2.0246 and hyperfine coupling to the ^{75}As ($I = ^3/_2$) and ^{31}P ($I = ^1/_2$) nuclei. The simulation afforded coupling constants of $A(^{75}As) = 21.7$ G, $A(^{31}P) = 42.2$ G, and $A(^{14}N) = 1.5$ G (not resolved), in excellent agreement with the EPR spectrum recorded in situ for the arsaphosphene radical anion [RAsPR]$^{-\cdot}$ (R = 2,6-(Mes)$_2$-4-MeC$_6$H$_2$), which afforded a similar "pseudo-sextet" pattern with $A(^{75}As) = 23$ G and $A(^{31}P) = 48$ G.[31] The calculated spin density is distributed symmetrically between the arsenic (0.39 *e*) and phosphorus atoms (0.31 *e*) with only little additional localization on each of the four nitrogen atoms (approx. 0.04 *e*, Figure 4, right).
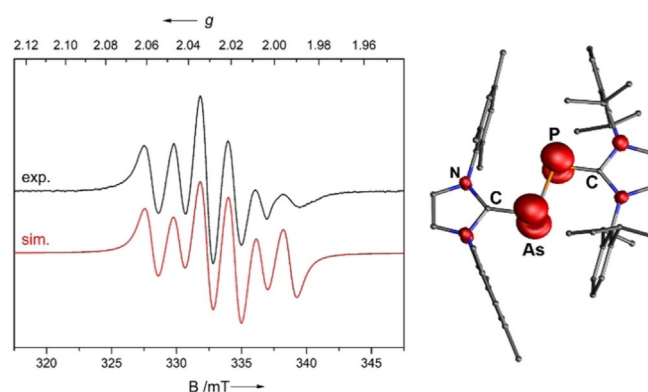

Figure 4. Left: Experimental (black) and simulated (red) EPR spectrum of [**5**]PF$_6$ in CH$_2$Cl$_2$ (298 K, 9.448437 GHz). Right: Spin-density distribution of radical [**5**]$^+$.

Further oxidation of **5**$^+$, or two-electron oxidation of **4**, furnished the dication [(IMes)AsP(IDipp)]$^{2+}$ (**6**$^{2+}$) however, it is also conveniently accessible from **3** through abstraction of the two chloride ions with two equivalents of gallium trichloride. This reaction was performed by addition of GaCl$_3$ to a THF solution of **3** at room temperature to afford [**6**][GaCl$_4$]$_2$ as a dark orange crystalline solid in 47 % yield after thorough washing with fluorobenzene and hexane (Scheme 1). The ^{31}P NMR spectrum of [**6**][GaCl$_4$]$_2$ gives rise to a characteristic lowfield resonance at 475.5 ppm (Figure S10, Supporting Information), which is in good agreement with the chemical shifts reported for homoleptic [(IDipp)P$_2$(IDipp)][OTf]$_2$ ($\delta = 452$ ppm)[10] and heteroleptic [(IMes)P$_2$(IDipp)][GaCl$_4$]$_2$ ($\delta = 438.5/440.1$ ppm $^1J_{PP} = 543$ Hz),[9] whereas arsaphosphenes of the type RAs=PR' (R, R' = aryl, alkyl) generally feature chemical shifts at even lower field (> 500 ppm).[32] It should be noted that the ^{1}H and ^{13}C NMR signals are sharper than those of **4**, revealing that rotation around the As—C and P—C bonds in **6**$^{2+}$ is faster on the NMR time scale, in agreement with a reduction of the corresponding bond orders (see below). The ^{13}C NMR spectrum exhibits two doublets for the carbene carbon atoms at 152.2 ($^1J_{PC} = 100$ Hz) and 151.3 ppm ($^2J_{PC} = 21$ Hz).

The molecular structures of [**5**]PF$_6$·CH$_2$Cl$_2$ and [**6**][GaCl$_4$]$_2$·2C$_6$H$_5$F were established by X-ray diffraction analyses; [**5**]PF$_6$·CH$_2$Cl$_2$ crystallizes with two independent molecules in the asymmetric unit, and ORTEP diagrams of all species are presented in the Supporting Information (Figures S22 and S23). Figure 5 shows an overlay of the structures of **4**, **5**$^+$, and **6**$^{2+}$, revealing that the *trans*-bent geometry and the nearly co-planar arrangement of the AsP unit and the imidazole planes in **4** is retained in the oxidized species. Upon oxidation, the As—P bond lengths decrease from 2.3149(8) in **4** to 2.2379(4)/2.2416(4) in **5**$^+$ and 2.1610(8) Å in **6**$^{2+}$, which is accompanied by an elongation of the As—C and P—C bonds (Table 1). The As—P bond in radical **5**$^+$ is slightly shorter than the corresponding bonds in the neutral radical [(IDipp)$_2$(μ-PAsP)] (2.256(1)/2.266(1) Å),[22] whereas this bond length in **6**$^{2+}$ corresponds to an As=P double bond (2.16 Å).[25] Consequently, similar, albeit slightly shorter As—P distances were found in arsaphosphenes of the type RAs=PR',[32,33] such as 2.125(1) Å for
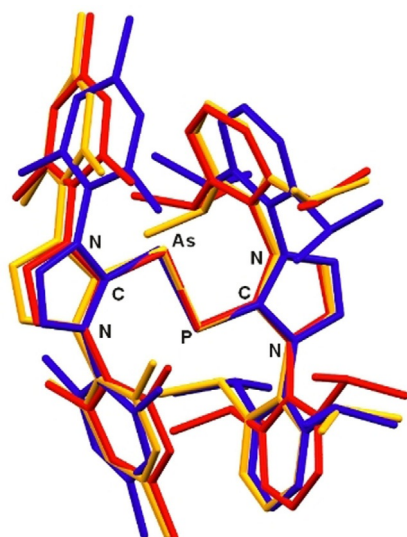
Figure 5. Overlay of the molecular structures of **4** (orange), **5**⁺· (blue), and **6**²⁺ (red). Pertinent bond lengths are assembled in Table 1. Selected torsion angles [°] in **4**: C-As-P-C 162.25(13), N-C-As-P 172.91(18), N-C-P-As 179.38(19); **5**·⁺ (molecule 1/molecule 2): C-As-P-C 171.04(7)/177.51(7), N-C-As-P 169.35(13)/177.46(12), N-C-P-As 177.89(11)/174.03(13); **6**²⁺: C-As-P-C 179.80(15), N-C-As-P 173.9(3) and N-C-P-As 175.2(2).

Table 1. Comparison of selected experimental (top) and calculated (bottom) bond lengths [Å] and associated Wiberg Bond Indices (WBI).

Comp.	As—P	WBI	As—C	WBI	P—C	WBI
4	2.3149(8) 2.356	1.02	1.883(2) 1.908	1.24	1.750(3) 1.772	1.35
5⁺·	2.2379(4)/ 2.2416(4) 2.288	1.22	1.9377(15)/ 1.9425(15) 1.957	1.02	1.7995(15)/ 1.8000(15) 1.810	1.13
6²⁺	2.1610(8) 2.216	1.63	1.959(3) 1.987	0.91	1.818(3) 1.837	1.02

R=CH(SiMe₃) and R′=2,4,6-tBu₃C₆H₂),[34] 2.141(5) Å for R=R′=2,4,6-tBu₃C₆H₂),[35] and 2.134(2) Å for R=(2,4,6-iPr₃C₆H₂)₂C₆H₃, and R′=Mes.[36] However, it should be noted that diarylarsaphosphenes just like the corresponding diphosphenes exhibit orthogonal orientations of the aryl groups towards the central dipnictene unit. A virtually identical As—P bond length of 2.161(1) Å was recently established for a cyclic *cis*-arsaphosphene.[26]

To assess the bonding situation further in the arsenic–phosphorus species **4**, **5**⁺·, and **6**²⁺, their structures were optimized by the density functional theory (DFT) method at the B97-D level of theory, followed by natural bond orbital (NBO) analysis. The computed structural parameters are in good agreement with those established by X-ray diffraction analysis, although consistently longer As—P, As—C and P—C bond lengths were obtained (Table 1). The shortening of the As—P bonds with consecutive elongation of the As—C and P—C bonds in the series **4**, **5**⁺·, and **6**²⁺ is accurately reproduced, and the increase of the Wiberg bond index (WBI) from 1.02 in **4** to 1.22 in **5**⁺·

and 1.63 in **6**²⁺ corroborates the gradual increase of the As—P bond order from single to double-bond character. This trend can be conveniently rationalized by analysis of the frontier molecular orbitals in **4**, **5**⁺·, and **6**²⁺ (Figure 6), revealing that the highest occupied molecular orbital in **4** represents mainly the antibonding π*(As—P) orbital, and stepwise oxidation with removal of electrons from this orbital will generate the singly occupied molecular orbital (SOMO) in **5**⁺· and lastly the lowest unoccupied molecular orbital (LUMO) in **6**²⁺.
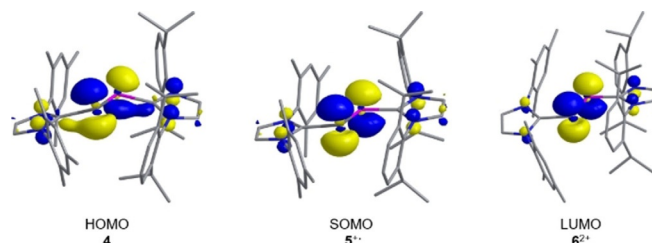

HOMO **4**   SOMO **5**⁺·   LUMO **6**²⁺

Figure 6. Frontier molecular orbitals in **4**, **5**⁺·, and **6**²⁺ with π*(As—P) character.

To the best of our knowledge, the arsenic monophosphide species [(IMes)AsP(IDipp)] (**4**), [(IMes)AsP(IDipp)]⁺· (**5**), and [(IMes)AsP(IDipp)]²⁺ (**6**) represent the first system, in which N-heterocyclic carbenes have been used for the stabilization of highly reactive heterodiatomic molecules containing two different heavier main-group elements. The heteroleptic set of NHC ligands allowed to establish the solid-state structures unequivocally by avoiding crystallographic disorder of the As and P atoms. The synthesis of this series built on a modular approach with (IDipp)PSiMe₃ (**1**) serving as the synthon for the introduction of low-valent phosphorus. With **1** and also the corresponding arsinidene adducts (NHC)AsSiMe₃ at hand,[29] numerous other heterodiatomic species of the type [(NHC)EE′(NHC)] (E=P, As; E′=Group 13, 14, 15 element) should be accessible.

Furthermore, the reactivity of [(IMes)AsP(IDipp)] (**4**) for example towards O₂ and N₂O to stabilize elusive arsenic–phosphorus oxide species,[37] and its potential to release the AsP molecule for applications in transition-metal chemistry and materials science will be investigated.[38]

Acknowledgements

Conflict of interest

The authors declare no conflict of interest.

[1] a) Y. Wang, G. H. Robinson, *Inorg. Chem.* **2011**, *50*, 12326–12337; b) Y. Wang, G. H. Robinson, *Dalton Trans.* **2012**, *41*, 337–345; c) D. J. D. Wilson, J. L. Dutton, *Chem. Eur. J.* **2013**, *19*, 13626–13637; d) V. Nesterov, D. Reiter, P. Bag, P. Frisch, R. Holzner, A. Porzelt, S. Inoue, *Chem. Rev.* **2018**, *118*, 9678–9842; e) A. Doddi, M. Peters, M. Tamm, *Chem. Rev.* **2019**, *119*, 6994–7112.

[2] H. Braunschweig, R. D. Dewhurst, K. Hammond, J. Mies, K. Radacki, A. Vargas, *Science* **2012**, *336*, 1420–1422.

[3] Y. Wang, Y. Xie, P. Wei, R. B. King, H. F. Schaefer III, P. von R Schleyer, G. H. Robinson, *Science* **2008**, *321*, 1069–1071.

[4] A. Sidiropoulos, C. Jones, A. Stasch, S. Klein, G. Frenking, *Angew. Chem. Int. Ed.* **2009**, *48*, 9701–9704; *Angew. Chem.* **2009**, *121*, 9881–9884.

[5] C. Jones, A. Sidiropoulos, N. Holzmann, G. Frenking, A. Stasch, *Chem. Commun.* **2012**, *48*, 9855–9857.

[6] Y. Wang, Y. Xie, P. Wei, R. B. King, H. F. Schaefer III, P. v. R. Schleyer, G. H. Robinson, *J. Am. Chem. Soc.* **2008**, *130*, 14970–14971.

[7] M. Y. Abraham, Y. Wang, Y. Xie, P. Wei, H. F. Schaefer III, P. v. R. Schleyer, G. H. Robinson, *Chem. Eur. J.* **2010**, *16*, 432–435.

[8] R. Kinjo, B. Donnadieu, G. Bertrand, *Angew. Chem. Int. Ed.* **2010**, *49*, 5930–5933; *Angew. Chem.* **2010**, *122*, 6066–6069.

[9] A. Doddi, D. Bockfeld, M.-K. Zaretzke, C. Kleeberg, T. Bannenberg, M. Tamm, *Dalton Trans.* **2017**, *46*, 15859–15864.

[10] O. Back, B. Donnadieu, P. Parameswaran, G. Frenking, G. Bertrand, *Nat. Chem.* **2010**, *2*, 369–373.

[11] M. Y. Abraham, Y. Wang, Y. Xie, R. J. Gilliard, Jr., P. Wei, B. J. Vaccaro, M. K. Johnson, H. F. Schaefer III, P. v. R. Schleyer, G. H. Robinson, *J. Am. Chem. Soc.* **2013**, *135*, 2486–2488.

[12] a) K. K. Yee, W. E. Jones, *J. Chem. Soc. Chem. Commun.* **1969**, 586a; b) L. Harding, W. E. Jones, K. K. Yee, *Can. J. Phys.* **1970**, *48*, 2842–2851; c) F. Leung, S. A. Cooke, M. C. L. Gerry, *J. Mol. Spectrosc.* **2006**, *238*, 36–41.

[13] M. Rasanen, L. A. Heimbrook, G. P. Schwartz, V. E. Bondybey, *J. Chem. Phys.* **1986**, *85*, 86–92.

[14] K. A. Gingerich, D. L. Cocke, J. Kordis, *J. Phys. Chem.* **1974**, *78*, 603–606.

[15] a) W. Klemm, I. V. Falkowski, *Z. Anorg. Allg. Chem.* **1948**, *256*, 343–348; b) I. Karakaya, W. T. Thompson, *J. Phase Equilib.* **1991**, *12*, 343–346; c) O. Osters, T. Nilges, F. Bachhuber, F. Pielnhofer, R. Weihrich, M. Schöneich, P. Schmidt, *Angew. Chem. Int. Ed.* **2012**, *51*, 2994–2997; *Angew. Chem.* **2012**, *124*, 3049–3052.

[16] a) Z. Zhu, J. Guan, D. Tománek, *Nano Lett.* **2015**, *15*, 6042–6046; b) F. Shojaei, H. S. Kang, *J. Phys. Chem. C* **2015**, *119*, 20210–20216; c) B. Liu, M. Köpf, A. N. Abbas, X. Wang, Q. Guo, Y. Jia, F. Xia, R. Weihrich, F. Bachhuber, F. Pielnhofer, Han Wang, R. Dhall, S. B. Cronin, M. Ge, X. Fang, T. Nilges, C. Zhou, *Adv. Mater.* **2015**, *27*, 4423–4429; d) J. Sun, N. Lin, H. Ren, C. Tang, L. Yang, X. Zhao, *Phys. Chem. Chem. Phys.* **2016**, *18*, 9779–9787; e) H. Shu, J. Guo, *Mater. Horiz. Mater. Res. Express* **2018**, *5*, 036302.

[17] J. E. Davies, L. C. Kerr, M. J. Mays, P. R. Raithby, P. K. Tompkin, A. D. Woods, *Angew. Chem. Int. Ed.* **1998**, *37*, 1428–1429; *Angew. Chem.* **1998**, *110*, 1473–1475.

[18] J. E. Davies, M. J. Mays, P. R. Raithby, G. P. Shields, P. K. Tompkin, A. D. Woods, *J. Chem. Soc. Dalton Trans.* **2000**, 1925–1930.

[19] B. M. Cossairt, C. C. Cummins, *J. Am. Chem. Soc.* **2009**, *131*, 15501–15511.

[20] B. M. Cossairt, M.-C. Diawara, C. C. Cummins, *Science* **2009**, *323*, 602.

[21] a) A. Doddi, D. Bockfeld, T. Bannenberg, P. G. Jones, M. Tamm, *Angew. Chem. Int. Ed.* **2014**, *53*, 13568–13572; *Angew. Chem.* **2014**, *126*, 13786–13790; b) M. Peters, A. Doddi, T. Bannenberg, M. Freytag, P. G. Jones, M. Tamm, *Inorg. Chem.* **2017**, *56*, 10785–10793.

[22] A. M. Tondreau, Z. Benkö, J. R. Harmer, H. Grützmacher, *Chem. Sci.* **2014**, *5*, 1545–1554.

[23] M. Balmer, H. Gottschling, C. von Hänisch, *Chem. Commun.* **2018**, *54*, 2659–2661.

[24] A. Hinz, M. M. Hansmann, G. Bertrand, J. M. Goicoechea, *Chem. Eur. J.* **2018**, *24*, 9514–9519.

[25] P. Pyykkö, M. Atsumi, *Chem. Eur. J.* **2009**, *15*, 12770–12779.

[26] M. Mehta, J. E. McGrady, J. M. Goicoechea, *Chem. Eur. J.* **2019**, *25*, 5445–5450.

[27] a) A. Hinz, A. Schulz, A. Villinger, *Chem. Eur. J.* **2016**, *22*, 12266–12269; b) A. Hinz, A. Schulz, A. Villinger, *Inorg. Chem.* **2016**, *55*, 3692–3699.

[28] A. J. Arduengo III, J. C. Calabrese, A. H. Cowley, H. V. R. Dias, J. R. Goerlich, W. J. Marshall, B. Riegel, *Inorg. Chem.* **1997**, *36*, 2151–2158.

[29] A. Doddi, M. Weinhart, A. Hinz, D. Bockfeld, J. M. Goicoechea, M. Scheer, M. Tamm, *Chem. Commun.* **2017**, *53*, 6069–6072.

[30] a) P. P. Power, *Chem. Rev.* **2003**, *103*, 789–810; b) C. D. Martin, M. Soleilhavoup, G. Bertrand, *Chem. Sci.* **2013**, *4*, 3020–3030.

[31] K. Tsuji, Y. Fujii, S. Sasaki, M. Yoshifuji, *Chem. Lett.* **1997**, *26*, 855–856.

[32] L. Weber, *Chem. Rev.* **1992**, *92*, 1839–1906.

[33] P. P. Power, *J. Chem. Soc. Dalton Trans.* **1998**, 2939–2951.

[34] A. H. Cowley, J. E. Kilduff, J. G. Lasch, S. K. Mehrotra, N. C. Norman, M. Pakulski, B. R. Whittlesey, J. L. Atwood, W. E. Hunter, *Inorg. Chem.* **1984**, *23*, 2582–2593.

[35] M. Bouslikhane, H. Gornitzka, J. Escudié, H. Ranaivonjatovo, *J. Organomet. Chem.* **2001**, *619*, 275–279.

[36] B. Twamley, P. P. Power, *Chem. Commun.* **1998**, 1979–1980.

[37] a) Y. Wang, Y. Xie, P. Wei, H. F. Schaefer, P. v. R. Schleyer, G. H. Robinson, *J. Am. Chem. Soc.* **2013**, *135*, 19139–19142; b) Y. Wang, M. Chen, Y. Xie, P. Wei, H. F. Schaefer III, P. v. R. Schleyer, G. H. Robinson, *Nat. Chem.* **2015**, *7*, 509–513.

[38] CCDC 1940130, 1940132, 1940133, and 1940134 contain the supplementary crystallographic data for this paper. These data are provided free of charge by The Cambridge Crystallographic Data Centre.